Naval Research Laboratory

Stennis Space Center, MS 39529-5004

NRL/MR/7320--16-9704

Are Hydrostatic Models Still Capable of Simulating Oceanic Fronts

YALIN FAN
ZHITAO YU

Ocean Dynamics and Prediction Branch
Oceanography Division

FENGYAN SHI

University of Delaware
Newark, Delaware

November 10, 2016

REPORT DOCUMENTATION PAGE

Form Approved
OMB No. 0704-0188

1. REPORT DATE *(DD-MM-YYYY)*	**2. REPORT TYPE**	**3. DATES COVERED** *(From - To)*
10-11-2016	Memorandum Report	

4. TITLE AND SUBTITLE

Are Hydrostatic Models Still Capable of Simulating Oceanic Fronts?

5a. CONTRACT NUMBER

5b. GRANT NUMBER

5c. PROGRAM ELEMENT NUMBER

6. AUTHOR(S)

Yalin Fan, Zhitao Yu, and, Fengyan Shi[1]

5d. PROJECT NUMBER

5e. TASK NUMBER

5f. WORK UNIT NUMBER
73-N2F5-05-5

7. PERFORMING ORGANIZATION NAME(S) AND ADDRESS(ES)

Naval Research Laboratory
Oceanography Division
Stennis Space Center, MS 39529-5004

8. PERFORMING ORGANIZATION REPORT NUMBER

NRL/MR/7320--16-9704

9. SPONSORING / MONITORING AGENCY NAME(S) AND ADDRESS(ES)

Naval Research Laboratory
Director of Research, Code 1001
4555 Overlook Avenue, SW
Washington, DC 20375

10. SPONSOR / MONITOR'S ACRONYM(S)

NRL

11. SPONSOR / MONITOR'S REPORT NUMBER(S)

12. DISTRIBUTION / AVAILABILITY STATEMENT

Approved for public release; distribution is unlimited.

13. SUPPLEMENTARY NOTES

[1]University of Delaware, Newark, DE

14. ABSTRACT

Sub-mesoscale structures such as oceanic fronts can play a very important role in the transfer of properties, tracers, momentum and energy between the surface ocean and the upper thermocline. The ability to correctly represent the fronts in ocean circulation models is important for mixed layer and thermocline simulations as well as large scale circulations.

Numerical experiments are conducted using hydrostatic (HY) and nonhydrostatic (NH) models to address the relevance of NH effects on the evolution of density fronts and the development of meso- and submeso-scale vertical motions. Model results indicate that even though the NH simulations give stronger upwelling/downwelling than the HY simulations, the characteristics of submesoscale structures are very similar between them, suggesting that the HY model are capable to produce correct dynamical response for oceanic fronts.

Model resolution is found to be critical for frontal simulations for both hydrostatic and nonhydrostatic models, and 100 meter resolution is adequate for frontal simulations.

15. SUBJECT TERMS

Non-hydrostatic modeling
Dynamic response of oceanic density fronts
Hydrostatic modeling

16. SECURITY CLASSIFICATION OF:			**17. LIMITATION OF ABSTRACT**	**18. NUMBER OF PAGES**	**19a. NAME OF RESPONSIBLE PERSON**
a. REPORT	**b. ABSTRACT**	**c. THIS PAGE**			Yalin Fan
Unclassified Unlimited	Unclassified Unlimited	Unclassified Unlimited	Unclassified Unlimited	23	**19b. TELEPHONE NUMBER** *(include area code)* (228) 688-4655

TABLE OF CONTENTS

FIGURE CAPTION

Abstract

Sub-mesoscale structures such as oceanic fronts can play a very important role in the transfer of properties, tracers, momentum and energy between the surface ocean and the upper thermocline. The ability to correctly represent the fronts in ocean circulation models is important for mixed layer and thermocline simulations as well as large scale circulations.

Numerical experiments are conducted using hydrostatic (HY) and nonhydrostatic (NH) models to address the relevance of NH effects on the evolution of density fronts and the development of meso- and submeso-scale vertical motions. Model results indicate that even though the NH simulations give stronger upwelling/downwelling than the HY simulations, the characteristics of submesoscale structures are very similar between them, suggesting that the HY model are capable to produce correct dynamical response for oceanic fronts.

Model resolution is found to be critical for frontal simulations for both hydrostatic and nonhydrostatic models, and 100 meter resolution is adequate for frontal simulations.

1. Introduction

Oceanic submesoscale structures usually have a horizontal scale of 1 to 10 km. They are inevitably crucial to bridging the meso and smaller scales (Thomas et. al. 2008). At the submesoscale, the nonhydrostatic process start to kick in, but may or may not be significant depending on what phenomenon we are looking at. Internal tides are examples where nonhydrostatic processes have significant influence, while the oceanic fronts can still be considered hydrostatic given their horizontal and vertical scales (Mahadevan 2006).

Fronts are very common to the ocean (Ullman and Cornillon 1999), and associated with narrow geostrophic jets and strong shear (Ferrari and Rudnick, 2000). Sub-mesoscale structures such as fronts are thought to be instrumental in transferring energy and properties from the largely adiabatic mesoscale flow field to a scale where mixing occurs (McWilliams 2003, Molemarker et al. 2005, Thomas et. al. 2008). They can facilitate the exchange of properties between the surface ocean and upper thermocline. The intensity of the frontal, up and down-welling motions will set the rates of exchange in the vertical, particularly beyond the reach of the mixed layer. The ability to correctly represent them in the ocean models is important for mixed layer and thermocline simulations as well as large scale circulations. The location of density fronts and the depth of mixed layer and thermocline are also very important for acoustic performance predictions.

Marshall et al (1997) argue that the hydrostatic models presumably begin to break down somewhere between 10 and 1 km resolution, as the resolved horizontal scale of the motion becomes comparable with its vertical scale. However, nonhydrostatic models have not shown much advantage on simulating oceanic fronts vs. hydrostatic models at

Manuscript approved October 6, 2016.

resolutions from 0.25 km to 1 km. Mahadevan (2006) argues that greater resolution is required to enter the regime where the differences become apparent. Although it is well established that higher resolution can produce more realistic modeling of small-scale features, the importance of grid resolution in the vicinity of strong density fronts has not yet been investigated. In this study, hydrostatic and nonhydrostatic models are used to simulate oceanic salinity fronts at resolutions range from 50 meters to 1km. The model details are given in section 2; section 3 outlines the design of numerical experiments conducted; in section4, the characteristics of the submesoscale motions are assessed in these simulations and the underlying mechanisms and conditions for the existence and evolution of the submesoscale, frontal processes and the vertical circulation associated with them are investigated; the conclusion is given in section 5.

2. Method

2.1 The Nonhydrostatic model

NHWAVE is a non-hydrostatic wave and circulation model developed at University of Delaware (Ma et al. 2012, Shi et al., 2015). Here, we only list the equations related to the present study. The incompressible Navier-Stokes equations can be written as

$$\frac{\partial u}{\partial t}+\frac{\partial uu}{\partial x}+\frac{\partial uv}{\partial y}+\frac{\partial uw}{\partial z}=-\frac{1}{\rho}\frac{\partial p}{\partial x}+g_x+\frac{\partial \tau_{xx}}{\partial x}+\frac{\partial \tau_{xy}}{\partial y}+\frac{\partial \tau_{xz}}{\partial z} \quad (1)$$

$$\frac{\partial v}{\partial t}+\frac{\partial vu}{\partial x}+\frac{\partial vv}{\partial y}+\frac{\partial vw}{\partial z}=-\frac{1}{\rho}\frac{\partial p}{\partial y}+g_y+\frac{\partial \tau_{yx}}{\partial x}+\frac{\partial \tau_{yy}}{\partial y}+\frac{\partial \tau_{yz}}{\partial z} \quad (2)$$

$$\frac{\partial w}{\partial t}+\frac{\partial wu}{\partial x}+\frac{\partial wv}{\partial y}+\frac{\partial ww}{\partial z}=-\frac{1}{\rho}\frac{\partial p}{\partial z}+g_z+\frac{\partial \tau_{zx}}{\partial x}+\frac{\partial \tau_{zy}}{\partial y}+\frac{\partial \tau_{zz}}{\partial z} \quad (3)$$

$$\frac{\partial u}{\partial x}+\frac{\partial v}{\partial y}+\frac{\partial w}{\partial z}=0 \quad (4)$$

where u(x, y, z, t), v(x, y, z, t), w(x, y, z, t) are flow velocity components, and **v** = (u, v, w); ρ is water density; p(x, y, z, t) is pressure; g_x, g_y, g_z are gravitational force components; τ_{ij}, (i, j) = x, y, z are turbulent stress components which can be modeled by a turbulence closure model. In the present study, the standard Smagorinsky LES model is used. The conservation equation for a passive tracer, for example, salinity S, can be written as

$$\frac{\partial S}{\partial t} + u\frac{\partial S}{\partial x} + v\frac{\partial S}{\partial y} + w\frac{\partial S}{\partial z} = \kappa_s \nabla^2 S \tag{5}$$

where κ_s is the diffusivity of salinity. The fluid density ρ is calculated from salinity and temperature based on the Equation of State of seawater. However, a constant temperature is used in the following test cases. The Boussinesq approximation is employed for formulating the baroclinic pressure in the momentum equations.

NHWAVE uses a combined finite-volume and finite-difference scheme with a Godunov-type method for the spatial discretization and a two-stage (second-order) Strong Stability-Preserving (SSP) Runge-Kutta scheme for the time integration. A two-step predictor-corrector projection method is applied to solve the dynamic pressure. The high performance HYPRE software library is used to solve the pressure Poisson equation. The model is parallelized with Message Passing Interface (MPI).

2.2 Modification to NHWAVE

NHWAVE is designed for coastal simulations with small domains. The earth rotation effect is not considered. To use NHWAVE for ocean front simulations, Coriolis effect is added to the model momentum equations:

$$\frac{\partial u}{\partial t} + \frac{\partial uu}{\partial x} + \frac{\partial uv}{\partial y} + \frac{\partial uw}{\partial z} - fv + \underbrace{bw} = -\frac{1}{\rho}\frac{\partial p}{\partial x} + g_x + \frac{\partial \tau_{xx}}{\partial x} + \frac{\partial \tau_{xy}}{\partial y} + \frac{\partial \tau_{xz}}{\partial z} \tag{6}$$

$$\frac{\partial v}{\partial t}+\frac{\partial vu}{\partial x}+\frac{\partial vv}{\partial y}+\frac{\partial vw}{\partial z}+fu=-\frac{1}{\rho}\frac{\partial p}{\partial y}+g_y+\frac{\partial \tau_{yx}}{\partial x}+\frac{\partial \tau_{yy}}{\partial y}+\frac{\partial \tau_{yz}}{\partial z} \quad (7)$$

$$\underbrace{\frac{\partial w}{\partial t}+\frac{\partial wu}{\partial x}+\frac{\partial wv}{\partial y}+\frac{\partial ww}{\partial z}}-\underbrace{bu}=-\frac{1}{\rho}\frac{\partial p}{\partial z}+g_z+\underbrace{\frac{\partial \tau_{zx}}{\partial x}+\frac{\partial \tau_{zy}}{\partial y}+\frac{\partial \tau_{zz}}{\partial z}} \quad (8)$$

Where $f \equiv 2\Omega \sin\phi$ and $b \equiv 2\,\Omega\cos\phi$ (ϕ is the latitude) are the components of Coriolis acceleration in the horizontal (x, y) and vertical (z) directions. Note that the Coriolis terms are based on the Cartesian coordinates with y pointing to north.

2.3 Hydrostatic model vs. Nonhydrostatic model

In the nonhydrostatic model, all terms in the incompressible Navier Stokes equations (4) – (8) are retained, while in the hydrostatic model, all the terms underlined by the curly brackets are neglected. The vertical velocity *w* is diagnosed from the continuity equation (4) in the hydrostatic model rather than obtained prognostically from equation (8) as the nonhydrostatic model does.

By reducing the vertical momentum equation to a statement of hydrostatic balance, the hydrostatic (HY) model differs from the nonhydrostatic (NH) model due to the exclusion of the nonhydrostatic pressure gradient, and the Coriolis acceleration terms that contain the component of the earth's angular velocity, 2Ωcosϕ, in a direction tangential to the surface of the earth. NHWAVE is coded to easily switch between HY and NH mode through input file specifications.

2.4 Geostrophic balance

Both HY and NH model experiments are initialized using geostrophic balance. If we separate the pressure p into its HY component p_{HY} and NH component p_{NH}, the geostrophic balance for the NH model can be written as

$$fv_g = \frac{\partial p_{HY}}{\partial x} + \gamma \frac{\partial p_{NH}}{\partial x} - R_o bw \tag{10}$$

$$-fu_g = \frac{\partial p_{HY}}{\partial y} + \gamma \frac{\partial p_{NH}}{\partial y} \tag{11}$$

$$bu_g = \frac{\gamma}{\delta} \frac{\partial p_{NH}}{\partial z} \tag{12}$$

where, γ is the ratio of NH to HY pressure variations, δ is the depth to length aspect ratio, and $R_o = U/\Omega L$ is the Rossby number. In the NH model, b is non-zero and $\gamma = \delta$. The HY case is obtained by setting $\gamma = 0$ and $b = 0$.

3. Numerical Experiments

NHWAVE is run in both HY and NH modes in four sets of experiments with the resolution of 500, 250, 100, and 50 meters respectively.

In all experiments, the model domain is set up to be 16 km in the east-west direction, 24 km in the north-south direction and 800 meters in the vertical direction. An idealized front is initialized using geostrophic balance as shown in Figure 1. Periodic boundary conditions are applied in the x direction.

The domain is initialized with a sharp lateral south-to-north (S-N) density gradient based on the variation of salinity in the upper layers, such that the southern half of the domain has lighter water. This front is representative of the deep, semi-permanent fronts that are observed in the ocean (Rudnick, 1996) and extends to a depth of 250 meters. The

vertical stratification is prescribed based on observed open ocean profile in the North Atlantic. It overlies a weakly stratified region and a nearly homogeneous deeper layer.

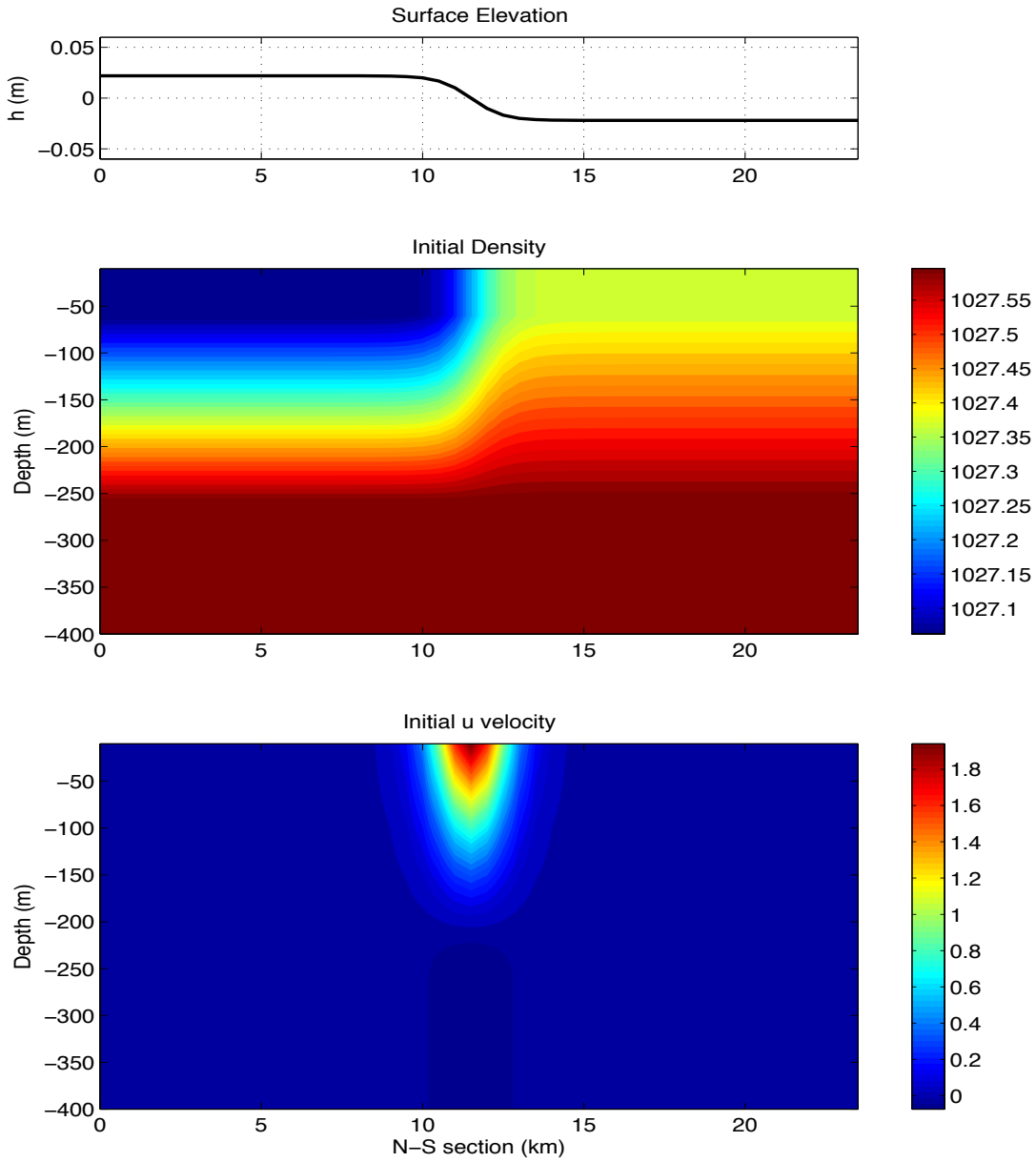

Figure 1. Across-channel cross section showing the sea surface elevation (top), potential density (middle) and along channel velocity in the upper 400 m that were used to initialize the model with an upper ocean front.

A S-N salinity variation is then superimposed on this vertical stratification. In the upper 50m $\Delta S = 0.2$psu; between 50m and 250m $\Delta S = 0.2(250-z)/200$, where z is the depth in m; and below 250m, there is no horizontal density variation. The salinity variation in the S-N direction is distributed according to $(\pm\Delta S/2)(1-\exp(-y_c/2))/(1+\exp(-y_c/2))$, where y_c is the distance in km from the channel center (northward is positive), and the ± sign are used according as y_c is positive or negative. The sea surface elevation is varied correspondingly over the same frontal region by 3.8cm, being higher in the southern region. Associated with the S-N density front is a west-to-east (W-E) geostrophic jet. The model velocities (and the NH pressure in the NH model) are initialized to satisfy the model's respective NH or HY balanced state as described in section 2.3. The model is allowed to evolve from this state into a meandering front, generating smaller scale features, when perturbed by weak winds. A constant westerly wind stress of 0.2Nm^{-2} (corresponding to 10m/s winds) is applied to the entire model domain continuously for 50 days.

4. Results

In this section, we analyze the numerical results to address the relevance of NH effects on the evolution of density fronts and the development of meso- and submeso-scale vertical motions. The numerical resolution required for modeling the vertical velocity at the fronts is also investigated. Based on these results, we will assess whether hydrostatic models are capable on simulating these features.

4.1 HY simulation with 500 m resolution

First, the evolution of the front is examined for the hydrostatic model with 500 m resolution. As the front evolves, the surface density field develops meanders. On day 31, submesoscale, vertical circulation cells are formed close to the surface along the boundary of the meandering front (Figure 2, upper panels). The vertical velocity field at both 20 and 70 meter depth show submesoscale features with the upwelling/downwelling velocities being stronger at 70 m depth where the base of the mixed layer is.

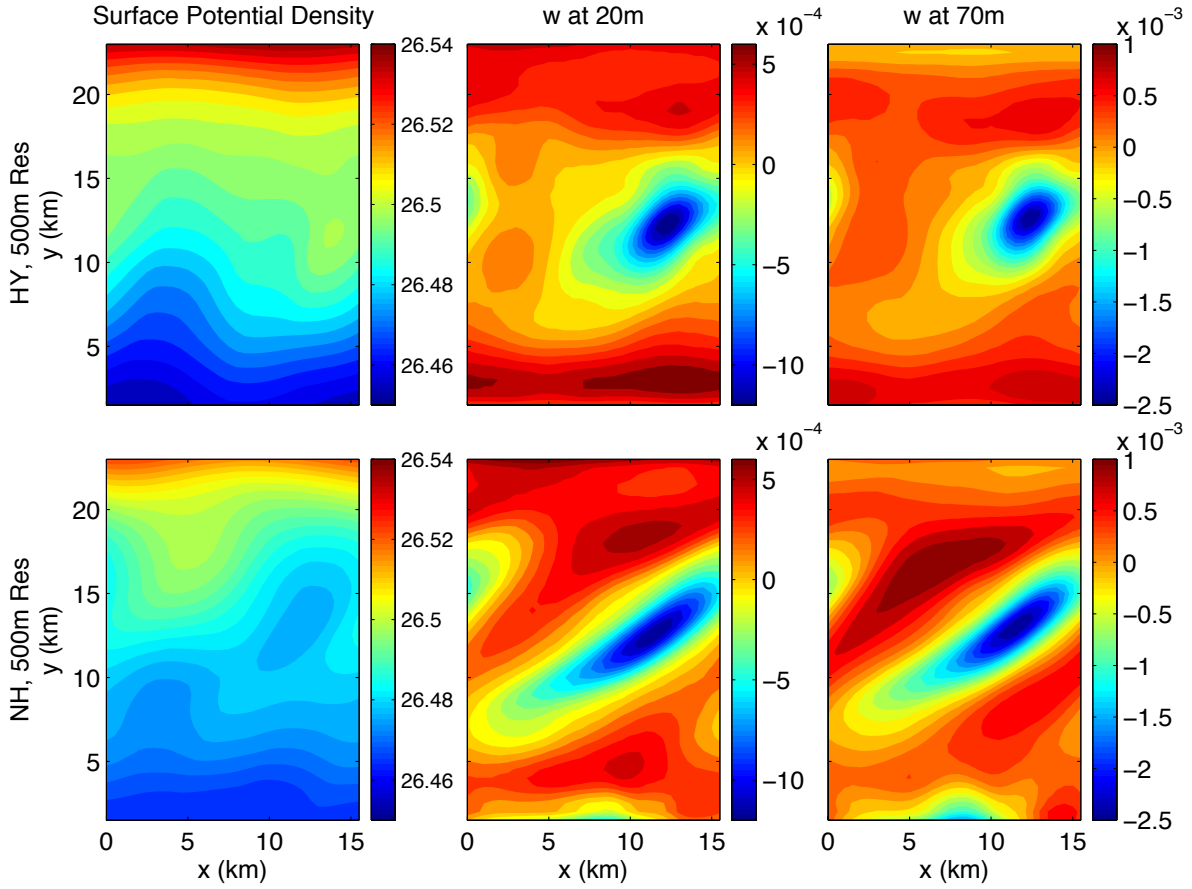

Figure 2. The surface density and the vertical velocity field (m/s) shown at 20 m and 70 m depth on day 31 from the HY (upper panels) and NH (lower panels) model forced with constant westerly wind stress of 0.2 N/m^2.

Stronger perturbation to the front is observed for the NH simulation. From the surface density plot, we can clearly see an eddy being formed and pinched off the meandering front. The magnitude of the upwelling/downwelling velocities have the similar magnitude as the HY simulation, but the submesoscale features in the vertical velocity field are elongated in the east-west direction. This may due to the fact that the growth rate for baroclinic instability in the NH and HY cases are different (Molemaker et. al. 2005).

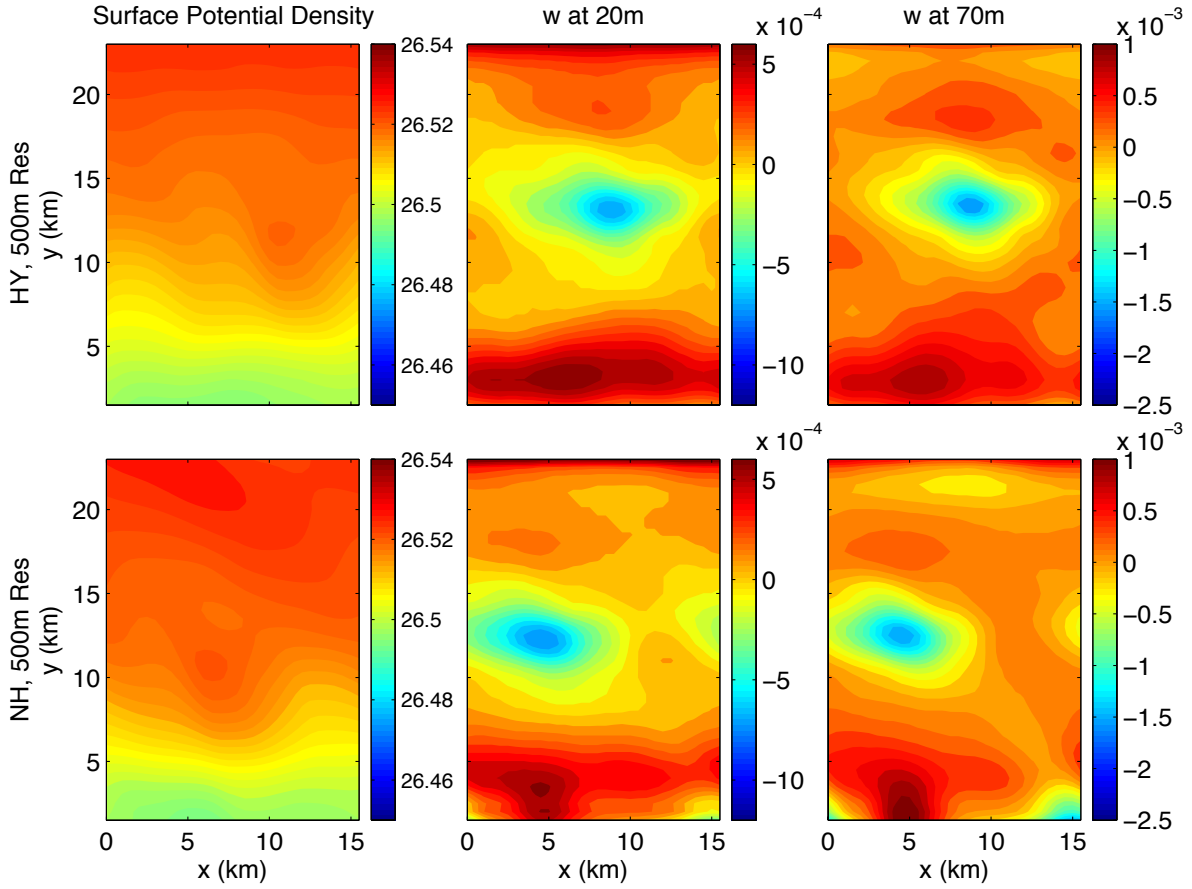

Figure 3. The surface density and the vertical velocity field (m/s) shown at 20 m and 70 m depth on day 50 from the HY (upper panels) and NH (lower panels) model forced with constant westerly wind stress of 0.2 N/m^2.

On day 50, the density and vertical velocity fields become very similar between the HY and NH simulations (Figure 3). The density gradients of the front are much smaller, and the upwelling/downwelling velocities are much weaker. The similarity between the HY and NH simulations suggests that these submesoscale features developed along the fronts are HY phenomenon or dominated by HY dynamics.

4.2 Comparison of HY and NH solutions at varies grid resolutions.

On account of the nonlinear evolution of the flow, the velocities and density distributions are different between the HY and NH simulations at 500 m resolution. However, it is difficult to identify characteristic differences between the NH and HY solutions. The differences between NH and HY models are more significant at the onset of baroclinic instability because the evolution of the instability differs between the two models (Mahadevan 2006). The wavy deformations of surface isopycnals tends to be more angularly oriented in the direction of the mean zonal flow in the NH case. But with time, the HY and NH solutions appear statistically similar. Thus, in Figure 4, frontal features from the NH and HY models at various horizontal resolution (500 m, 250 m, and 100 m) are compared at an earlier stage of the simulation (5 days).

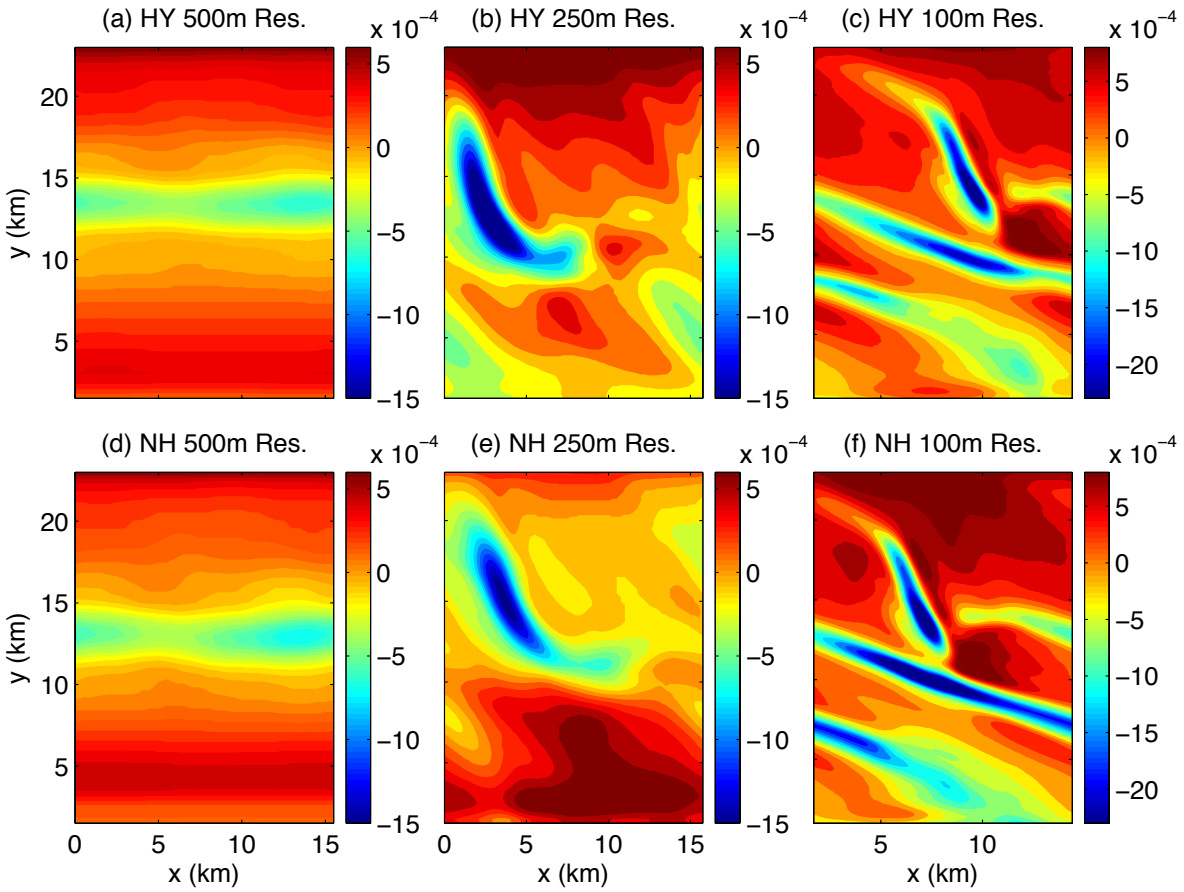

Figure 4. The near surface vertical velocity at the upper ocean front 5 days after model initialization in the NY and NH models at grid resolution of 500, 250, and 100 m. The color bar show the magnitude of w in m/s. Note that the range of color bar for (c) and (f) are larger due to the stronger upwelling/downwelling in the 100m resolution simulations.

Instability seems to develop much slower at lower resolution (500 m). Only weak meanders along the front are observed at day 5 for both the HY and NH simulations. The structure and magnitude of the near surface vertical velocity are very similar between them. When the resolution is doubled (250 m), submesoscale structures start to develop. Large areas of upwelling are accompanied by long strips of stronger downwelling along the edges of the meandering front where outcropping surface isopycnals are. The

upwelling/downwelling velocities are at the similar magnitude for the HY and NH simulations. Although the strong upwelling regions appear at different locations due to the random nature of the instability, the results are not considered statistically different between the HY and NH simulations.

As we increase the model resolution to 100 m, more submesoscale structures are observed. The width of the downwelling zone is narrower and sharper, and their magnitude increased by more than 30% compare to the 250 m resolution simulations. The NH simulation gives stronger upwelling/downwelling velocities than the HY simulation, but the HY simulation can still produce the similar dynamical structure as the NH simulation. Further increase the resolution to 50 m does not alter the results much (not shown), suggesting that the frontal submesoscale features can be adequately resolved at 100 m resolution.

The domain wide maximum surface upwelling/downwelling velocities from the NH and HY model runs at 250m and 100m resolution are compared in Figure 5. The region considered excludes a strip along the solid northern and southern boundaries of the domain, where upwelling is seen due to boundary effects.

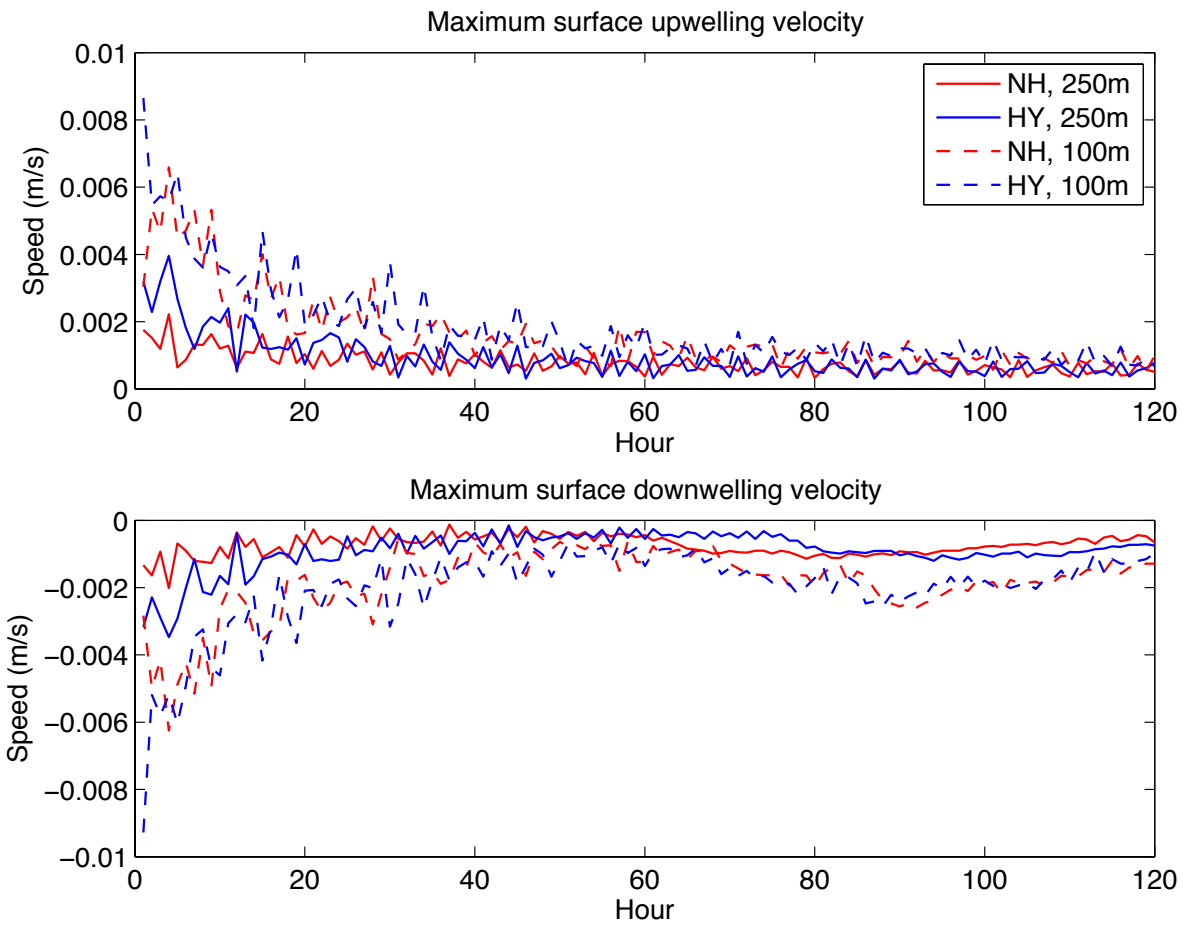

Figure 5. The maximum surface upwelling/downwelling velocity plotted against time for the 250m and 100m resolution simulations for both HY and NH models. Downwelling is more intense than upwelling, and increasing grid resolution increases the most intense downward velocities.

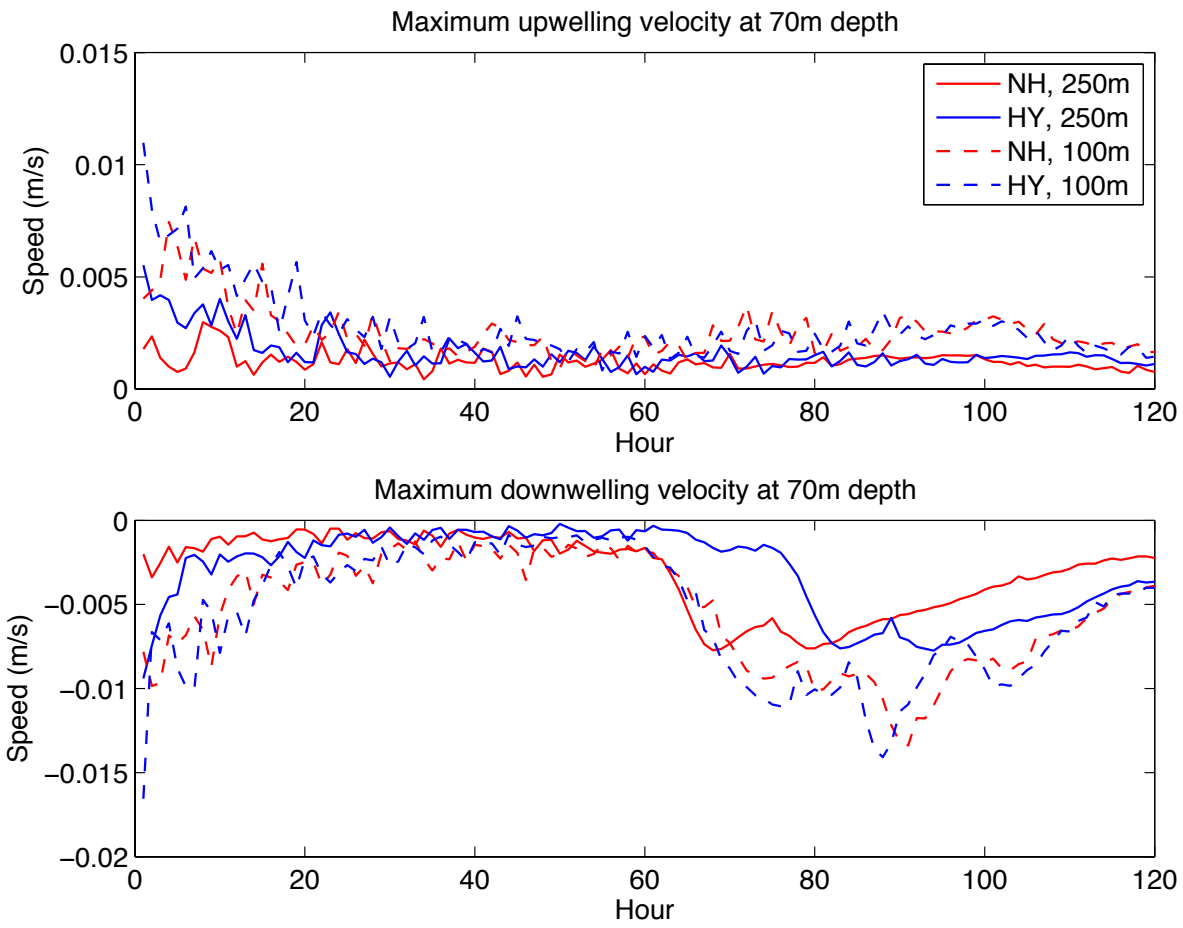

Figure 6. The maximum upwelling/downwelling velocity at 70m depth plotted against time for the 250m and 100m resolution simulations for both HY and NH models.

NH models start to develop instability earlier than HY models, but the magnitude of the disturbance eventually converge between the HY and NH models in time. Thus, after many days of model simulations, it is difficult to find systematic differences in the vertical velocities between the NH and HY models. Also notice that the variation of downwelling maxima at the mixed layer base show big difference between HY and NH simulations for both resolutions.

At the ocean surface, the downwelling maximum become more intense with increasing grid resolution, but the upwelling maxima are not affected by the model resolution much except during the first 20 hours or so. While at the base of the mixed layer (~70m depth), both upwelling and downwelling maxima are affected by model resolution. The higher resolution simulations give stronger upwelling/downwelling (Figure 6).

5. Discussion and Conclusion

Sub-mesoscale structures such as fronts can play a very important role in the transfer of properties, tracers, momentum and energy between the surface ocean and the upper thermocline. They are thought to be crucial in bridging the meso and smaller scales (Thomas et. al. 2008). The ability to correctly represent the fronts in ocean circulation models is important for mixed layer and thermocline simulations as well as large scale circulations. Since they are not fully three-dimensional and nonhydrostatic, it is important to address the question whether they can be adequately simulated in hydrostatic models due to the fact that hydrostatic ocean circulation models are still the most widely used tool in the ocean community.

In this study, numerical experiments are conduced using hydrostatic (HY) and nonhydrostatic (NH) models on the response of oceanic fronts to surface wind forcing to provide a descriptive picture of submesoscale, frontal processes and the vertical circulation associated with them. Model results indicate that even though the NH simulations give stronger upwelling/downwelling than the HY simulations, the characteristics of submesoscale structures are very similar between them, suggesting that the HY model are capable to produce correct dynamical response for oceanic fronts. Model resolution is found

to be critical for frontal simulations for both hydrostatic and nonhydrostatic models, and 100 meter resolution is adequate for frontal simulations.

Further study of the frontal processes is limited by the MPI design of NHWAVE. Although it supports multi CPU computations, the model grid is only decomposed in the horizontal. Thus the number of CPUs can be used are constrained by the number of horizontal grid points. Our tests suggest that one CPU need to have about 100 horizontal grid points in order to optimized the model speed for the chosen model grid. Further increase CPU numbers will actually slow down the model due to increased communications among CPUs. Also, the scale of this model is poor. Increase model domain size by 4 times will slow down the model by more than 10 times. For example, the NH experiment with 100m resolution can only compute ~6 physical hours in 1 day. These limitation has tremendously slowed down our experiments and forced us to use very small model domains. As a result, we can only resolve about half a wave length across the front, which makes it impossible for us to further analyze the mechanisms underlie the formation of the mesolscale motions, for example: what set the length scale of the mesoscale structures and affect their distribution in space and time, and what affect the intensity of the vertical velocity, etc.

Reference:

- Ferrari, R., Rudnick, D.L., 2000. The thermohaline structure of the upper ocean. Journal of Geophysical Research 105, 16,857–16,883.
- Ma, G., F. Shi, and J. T. Kirby, 2012: Shock-capturing non-hydrostatic model for fully dispersive surface wave processes. Ocean Modelling, 43-44, 23-35
- Mahadevan, A., 2006: Modeling vertical motion at ocean fronts: Are nonhydrostatic effects relevant at submesoscales? Ocean Modelling, 14, 222-240.
- Marshall, J., C. Hill, L. Perelman, and A. Adcroft, 1997: Hydrostatic, quasi-hydrostatic, and nonhydrostatic ocean modeling, J. Geophysical Research, 102, 5733 – 5752.
- McWilliams, J.C., 2003. Diagnostic force balance and its limits, Nonlinear Processes in Geophysical Fluid Dynamics. Kluwer Academic Publishers., pp. 287–304.
- Molemaker, M. J., McWilliams, J. C., Yavneh, I., 2005: Baroclinic instability and loss of balance. J. Physical Oceanography, 35, 1505 – 1517.
- Rudnick, D. L., 1996: Intensive surveys of the Azorres front. Part II: Inferring the geostrophic and vertical velocity fields. Journal of Geophysical Research 101 (C7), 16291 – 16303.
- Shi, J., F., Shi, J. T., Kirby, G., Gu, and G., Ma, 2015: Pressure decimation and interpolation (PDI) method for a baroclinic non-hydrostatic model, Ocean Modelling, 96, 265-279.
- Thomas, L. N., A. Tandon, and A. Mahadevan (2008), Submesoscale processes and dynamics, in Eddy Resolving Ocean Modeling, Geophys. Monogr. Ser., vol. 177, edited

by M. W. Hecht and H. Hasumi, pp. 17–38, AGU, Washington, D. C., doi:10.1029/177GM04.

- Ullman, D.S., Cornillon, P.C., 1999. Satellite-derived sea surface temperature fronts on the continental shelf of the northeast US coast. Journal of Geophysical Research 104 (C10), 23459–23478.